EXPERIMENTAL STUDY OF EVAPORATED $BaTiO_3$ FILMS

NASA TTF-9333

Eiji Sekine and Hiroo Toyoda

Journal of the Vacuum Society of Japan,
Vol. 5, No. 8, pp. 310-322, 1962

NATIONAL AERONAUTICS AND SPACE ADMINISTRATION
WASHINGTON D.C. MAY 1965

EXPERIMENTAL STUDY OF EVAPORATED $BaTiO_3$ FILMS*

Eiji Sekine and Hiroo Toyoda
(Received July 10, 1962)**

ABSTRACT

The films of $BaTiO_3$ and (Ba-Sr) TiO_3 were prepared /310*** with two types of evaporating methods. Several kinds of materials were used as substrates and their temperatures ranged from 200° C. The films were baked at various temperatures in air or O_2. The crystallization was investigated bymmeans of X-ray diffraction and electro-microscope. For the case of platinum substrate, the crystallization was not appreciable for the substrate temperatures and also baking temperature up to 400° C; thereabove, the crystalline size increased with the rise of temperature. The films, as they were evaporated, had low specific resistance and low dielectric constant and baking them brought about an increase in these two values. A (Ba_{0-95} Sr_{0-05}) TiO_3 film, thus baked at 1200° C, had a dielectric constant about 1500 at room temperature, and dielectric anomalies were observed at the temperatures 100, 0, and -80° C.

---

* Presented at the Joint Gen'l Meeting of Applied Physics, March 31, 1962.

** Electrical Communication Laboratory, Nippon Telegraph and Telephone Public Corporation, Musashino, Tokyo.

*** Note: Numbers in the margin indicate pagination in the original foreign text.

1. Introduction

Research on ferroelectric thin films was initiated in 1955 with the experimental study of evaporated $BaTiO_3$ films by Feldman (Ref. 1). Since that time, experiments by Moll (Ref. 2), Lure (Ref. 3), and others (Ref. 4 and Ref. 5) have been reported. Due to the need for miniaturization of parts with the advance of electronics, ferroelectric thin films are expected to have possibilities as nonlinear elements, memory elements, condenser materials, etc. Films evaporated in a vacuum for these purposes have many advantages, i.e., they are very thin, homogeneous, etc. The evaporation mechanism and the recrystallization process of compound oxides are of interest in physical terms. They have been investigated experimentally at some university laboratories (Ref. 6, Ref. 7, Ref. 8) in our country, because of the interest in the relationship with a crystalline surface layer of $BaTiO_3$. Up to the present, few experimental results have been obtained, however. In addition, the phenomena are complicated and show different tendencies in different cases. Hence there is no established theory for their structure and properties as yet.

The single crystal and ceramic made of $BaTiO_3$ have been widely investigated in detail for the crystalline structure, electrical properties, etc. It is, therefore, reasonable to choose this material as the evaporated film of ferroelectric material. As a fundamental experiment with evaporated films using X-rays, we have observed the manner in which the evaporation conditions and the treatment after evaporation affect the formation of the $BaTiO_3$ thin film. We also measured its resistance and dielectric constant. In addition, we have considered some problem areas to be treated in the future.

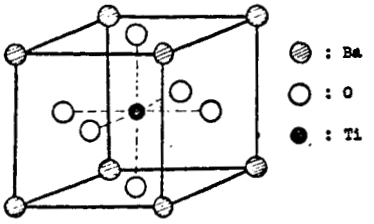

Figure 1

Cubic Perovskite-type Structure of $BaTiO_3$.

For convenience in explaining the properties of evaporated $BaTiO_3$ films, the $BaTiO_3$ crystal is explained briefly as follows: $BaTiO_3$ has a structure of the perovskite type as shown in Figure 1. The temperature dependence of its lattice parameters is shown in Figure 2.

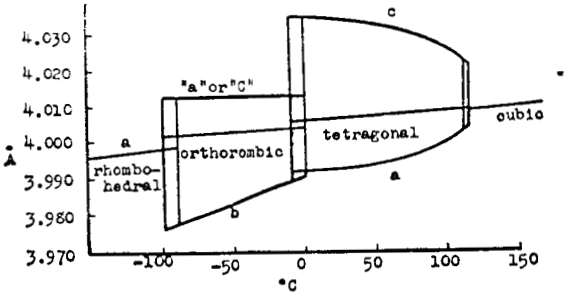

Figure 2

Lattice Parameters of $BaTiO_3$ as a Function of Temperature (After Kay and Vousden [Ref. 15]).

There are three transformation points: the first one lies at 120°C. Above this temperature, the crystal has a cubic phase. Between 120°C and the second transformation point, 0°C, it has tetragonal phase, with c/a = 1.01 at room temperature. Between 0°C and the third transformation point, -80°C, it has orthorhombic phase. Below the third point, the /311 phase is rhombohedral. The point 120°C is the Curie point, below which

spontaneous polarization is set up along the c-axis, and ferroelectricity appears. The temperature dependence of the dielectric constant (ε) of single crystals is shown in Figure 3.

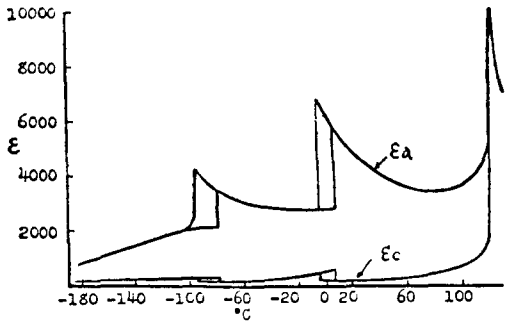

Figure 3

Dielectric Constant of $BaTiO_3$ Single Crystals.
(After Merz [Ref. 16]).

Since $BaTiO_3$ ceramic is composed of randomly-aligned fine single crystallites, all properties are averaged ones. It is known that slight differences in composition, impurities, baking conditions, etc. affect its properties considerably. For the solid solution (Ba·Sr)TiO_3, in which Ba is replaced by Sr, the Curie point shifts to a lower temperature as the doping amount of Sr increases. The phase equilibrium diagram of the BaO-TiO_2 system is shown in Figure 4.

2. Experimental Conditions

2.1 Evaporation Apparatus

The experimental apparatus for evaporation is shown briefly in Figure 5. The equipment consisted of a metallic bell jar of 40 cm in diameter, containing a tungsten heater (W) as the evaporation source, a substrate supporter and a heater, a funnel for $BaTiO_3$ powder, its vibrator,

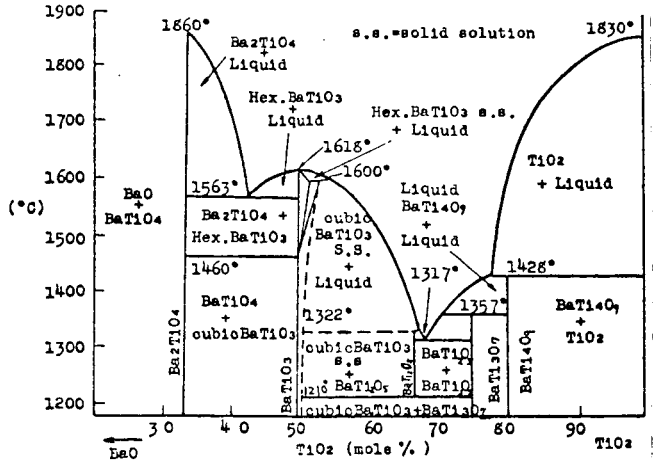

Figure 4

Phase Equilibrium Diagram of the BaO-TiO_2 System (After Rose and Roy [Ref. 17]).

a belt, a shutter, etc. The powder is dropped onto the belt by vibrating the plate attached under the funnel electromagnetically. The belt is driven by a motor outside the bell jar. The amount of material supplied to the evaporation heater is controlled by changing the speed of revolution of the belt and the frequency of the vibrator. The vacuum pressure attained by this apparatus is $1 \sim 2 \times 10^{-5}$ mmHg.

We used the following two evaporation methods:

(A) The powder is placed on the boat-shaped tungsten heater and evaporation is performed by heating it gradually. (This is designated as Method A.)

(B) A small amount of the powder is dropped on to the pre-heated tungsten heater and evaporated almost instantly. (This is designated as Method B.)

The heater temperature was set at $2,000^{o} \sim 2,200^{o}$C. Two steps were involved: in the beginning, the time required to attain $2,000^{o}$C was

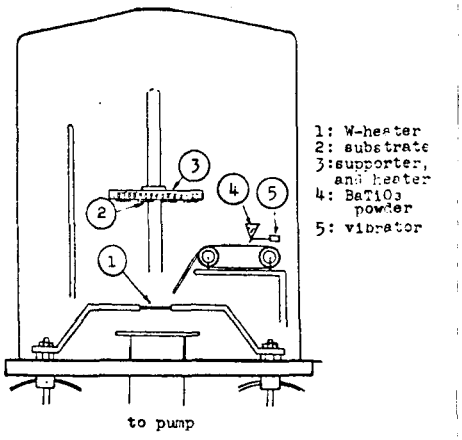

Figure 5

Experimental Apparatus for Evaporation.

about 20 seconds in Method A. Afterwards, it was shortened by im- /312
proving the heating power source, and we were able to heat to 2,200°C in about 5 seconds. The samples for the following X-ray analysis experiments were obtained by heating to 2,000°C in 20 seconds. The samples for the other experiments were obtained by heating to 2,200°C in 5 seconds.

2.2 Materials

For evaporation materials, we used powdered $BaTiO_3$ in single-crystal form, obtained by the Remeika method (K. F. method), and we also used $(Ba \cdot Sr)TiO_3$ solid solution ceramic powder, which contained 2 ~ 20% Sr.

2.3 Substrate Material and Temperature

For substrate material, we used platinum plate, glass plate, quartz glass plate, mica, alumina ceramic, nickel plate, etc. Before it was used, the platinum plate was treated with concentrated hydrochloric acid and heat-treated with a gas-burner. We used glass substrates and quartz

glass substrates, after dipping them in a concentrated mixture of chromic and sulphuric acid, washing them repeatedly in water, and then in alcohol.

The substrate temperature ranged from 200° to 1,200° C. The baking temperature after evaporation was 200° C - 1,200° C, and duration of baking was 30 minutes - 4 hours.

3. Experimental Results

Observations and measurements were carried out as follows. We observed the macroscopic structure of the obtained films, and the effect of substrate materials and baking temperature on the process of crystallization, optically and with an X-ray technique. In each procedure, electric resistance, optical density, and dielectric constant of the sample were also measured.

Upon observing the appearance during evaporation, we found that in method A the powder dissolved at 1,600° ~ 1,700° C, spread over the heater surface, and then evaporated gradually as the temperature of the tungsten heater increased gradually.

In method B, when the powder was dropped on the preheated heater, it was observed that fine particles evaporated instantly, but a drop of particles in a group did so in a similar manner to method A, but not instantly. A part of the powder was ejected in the form of clusters, but its effect on the substrate was considered to be small, since the distance between the heater and the substrate was more than 10 cm. After evaporation, we sometimes found a black-gray residue on the tungsten heater. This was assumed to be the reduced $BaTiO_3$ which was not evaporated, or a product resulting from reaction with tungsten.

The thickness of the evaporated film was calculated by weighing the evaporated amount on the platinum plate. For glass and quartz glass plates, we measured the thickness by using an interferometer. The density of $BaTiO_3$ ceramic is different for different baking conditions. It is about 5.5 for one baked at 1,300° C. For evaporated films, there was good agreement between thethickness determined by weighing the amount of evaporated substance and the thickness determined optically, if we set the density equal to 5.1. The film thickness in this experiment ranges from 1 μ to 3 μ.

3.1 External Appearance

The conditions of evaporation for both methods A and B are as follows: Platinum, glass and quartz glass are used as substrates. The substrate temperatures are 200°, 300°, 400° and 500° C. Baking after evaporation was performed in air at 200°, 300°, 500°, 600°, 700°, 800°, 1,000°, and 1,200° C. Duration of baking was about 30 minutes. It should be noted here that we increased the baking temperature of one sample after observing it under a microscope.

Immediately after the films were exposed to air after evaporation, they were transparent in both methods (A, B), although the degree of coloring differed in the two methods. The color of the film varied slightly with its thickness. The external appearance of the films is shown in Table 1. As time goes on, most of the films obtained by method A become dark, and are seen to have an uneven surface. In method B, however, such a time variation is not found. The cause of such a tendency in method A is assumed to be the following: during evaporation, a part of $BaTiO_3$ is resolved into BaO and TiO_2 and evaporated. When the film is exposed to

TABLE 1.

Method	A		B	
Substrate	Pt.	glass	Pt.	glass
Sub. Tem. °C	pale purple	pale purple	pale brown	pale brown
200	(S)	(S)	(T)	(T)
300	purplish green (S)	purple (S)	dark purple (T)	pale brown (T)
400	yellowish brown (S)	pale brown (S)	dark purple (T)	pale brown (T)
500	dark purple (S)	dark gray (S)	dark purple (T)	pale brown (T)

(S) : smoky (T) : transparent

air, $BaCO_3$ is produced through reaction with the CO_2 gas, which is accompanied by peeling and cracks on the film, which are secondary effects. For both methods, the reduction of $BaTiO_3$ and TiO_2 is assumed to be one of the causes of the complicated variation in coloring.

Observing the appearance of the film surface with a microscope, in the case of method A with glass and platinum substrates, we can see the circular or spiral pattern as shown in Figure 6 (a), (b). On the other hand, in the case of method A with quartz glass substrates and in the case of method B, with three kinds of substrate (glass, platinum and quartz glass), this pattern cannot be seen. Almost straight cracks are seen [Figure 6 (c) - (f)]. In the case of method A, the stripe-pattern on the film surface breaks up as time passes, and unevenness appears on the part which was smooth initially (Figure 7). In the /313 case of method B, however, such a time-dependent variation is not found. In the later experiment, even in method A, comparatively stable films were obtained, if the tungsten heater power was increased, and the material was evaporated in a shorter time. It follows from this that the effect

×100

(a) M : A
S : glass
S.T: 300°C
untreated

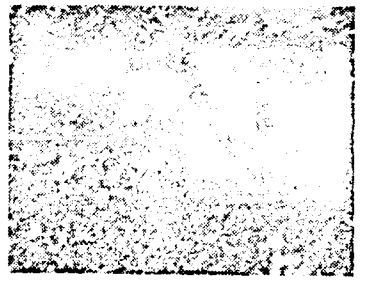

×100

(b) M : A
S : Pt
S.T: 300°C
untreated

×100

(c) M : A
S : quartz
S.T : 400°C
untreated

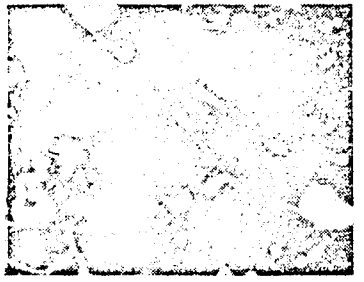

×100

(d) M : B
S : quartz
S.T: 200°C
untreated

×100

(e) M : B
S : quartz
S.T : 300°C
untreated

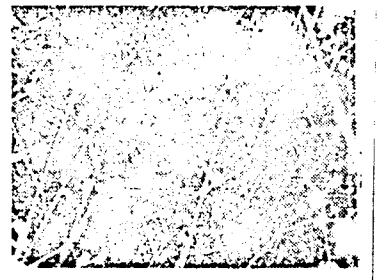

×100

(f) M : B
S : Pt
S.T : 500°C
untreated

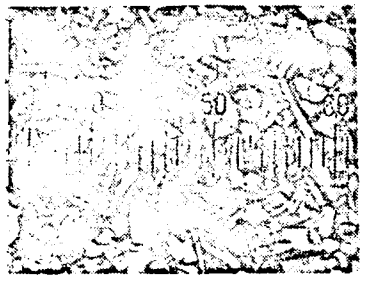

×350

(g) M : B
S : Pt
S.T: 300°C
B.T: 1200°C

Figure 6

Photomicrograph of Evaporated $BaTiO_3$ Films

Method (Hereafter Abbreviated as M.)
Substrate (as S.)
Substrate Temperature (as S.T)
Baking Temperature (as B.T)

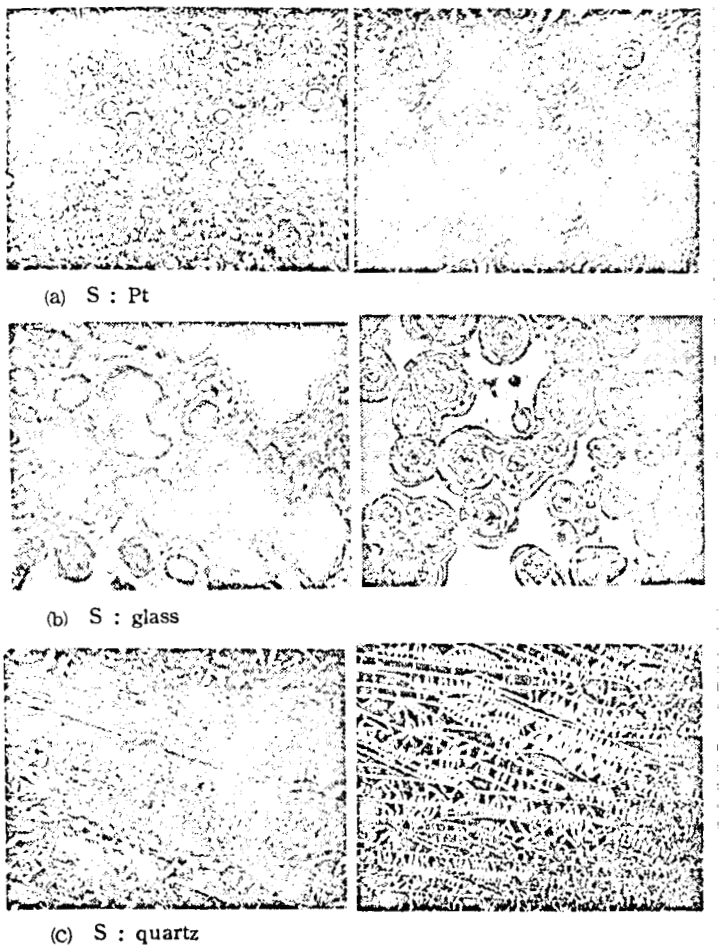

Figure 7

The Change of Surface Appearance of the Films Evaporated on to Three Different Substrates. The Left Column Shows the States Just After the Evaporation and the Right One Those After a Month in the Atmosphere.

of the evaporation rate on the film properties is considerable.

As the baking temperature is increased in air, the color of the film surface changes gradually. At 500° C, it becomes almost white or pale yellow, and above it there is no great change in the color. At 1,000° - 1,200° C, it becomes almost pale yellow or grayish yellow. As the baking temperature is further increased, cracks and peeling often appear on the film surface. The grain size is seen to become larger when the film is baked at 1,200° C [Figure 6 (g)].

3.2 X-ray Observations

The same samples, which were used for the optical microscope measurement, were observed by X-rays. They were measured with a diffraction meter at room temperature. The measuring conditions were as follows:

Target Material:	Cu	Filter Material:	Ni
Voltage:	35 KV	Current:	15mA
Scanning Speed:	1^{o}/min		

The diffraction angle, 2θ is observed between 10^{o} and 50^{o}, within which the diffraction intensity of $BaTiO_3$ is strong. The diffraction lines for (100), (110), (111) and (200) orientations are included within this angle range. The change in the diffraction intensity with the /314 advancement of recrystallization is measured at a diffraction line, $2\theta = 31.6^{o}$ or the (110) direction. Around this angle, there are many lines such as $BaTiO_3$ in a cubic crystal; $2\theta = 31.3^{o}$ for hexagonal $BaTiO_3$; 31.3^{o} for $BaTi_3O_7$; 30.05^{o} for $BaTi_4O_9$; and 29.75^{o} for $BaTi_2O_5$. Therefore, it is difficult to separate them from each other. However, it is reasonable to take the line of $2\theta = 31.6^{o}$ as a reference line, because the line of $2\theta = 31.6^{o}$ is always accompanied by the lines of $2\theta = 22^{o}$ (100), 38.9^{o} (111), and 45.35^{o} (200) in the cubic $BaTiO_3$ crystal. Sometimes rather sharp diffraction lines are seen at $2\theta = 39.7^{o}$ and 46.3^{o}. They are assumed to be due to the large crystal grains of the platinum plate used as a substrate.

First of all, some parts of the diffraction spectrum for the samples with the platinum substrate are shown. The spectrum of a sample treated by method A, in which the substrate temperature is 200^{o} C and no heat treatment is applied after the vacuum evaporation, is shown in Figure 8. The evaporated film seems to be amorphous, and the $BaTiO_3$ crystal is not

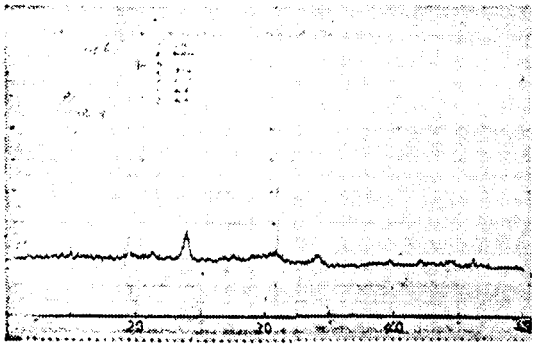

Figure 8

X-ray Diffraction Pattern of Evaporated BaTiO Film

M: A S: Pt
S.T: 200°C Untreated

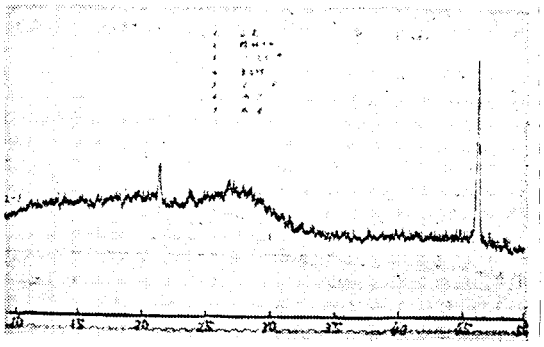

Figure 9 /315

X-ray Diffraction Pattern

M: B S: Pt
S.T: 200°C Untreated

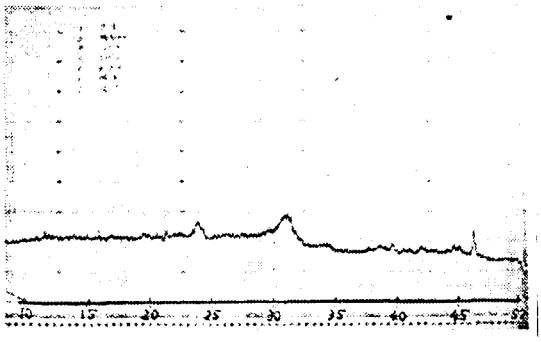

Figure 10

X-ray Diffraction Pattern

M: A S: Pt
S.T: 200°C B.T: 500°C

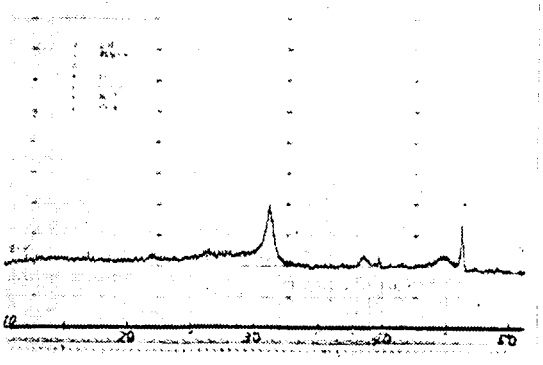

Figure 11

X-ray Diffraction Pattern

M: B S: Pt
S.T: 200°C B.T: 500°C

observed on the pattern. Only one line, which may correspond to a $BaCO_3$ crystal, can be observed. In the case of method B, shown in Figure 9, neither the $BaTiO_3$ crystal nor the $BaCO_3$ crystal can be observed. This is different from method A.

When the samples are heat-treated at 500° C, the diffraction pattern of $BaTiO_3$ can be observed. This is shown in Figures 10 and 11. The sample

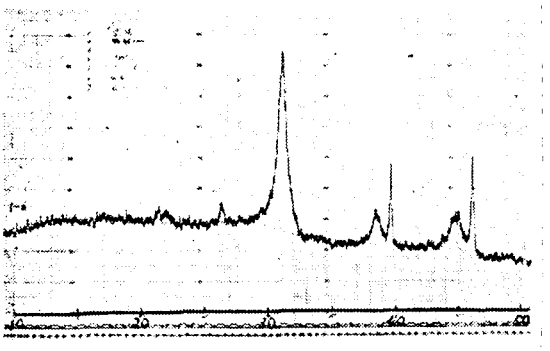

Figure 12

X-ray Diffraction Pattern

M: A S: Pt
S.T: 200°C B.T: 700°C

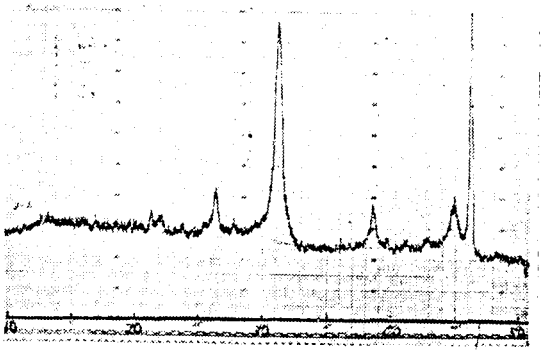

Figure 13

X-ray Diffraction Pattern

M: B S: Pt
S.T: 200°C B.T: 700°C

obtained by method A has a less intense and broadened diffraction line for $BaTiO_3$, as compared to the sample obtained by method B. By increasing the treatment temperature, the patterns become clear and the difference between these methods is barely apparent. This is shown from Figures 12 to 15. By increasing the substrate temperature to 300° C and 400° C, the results are almost the same as the case of 200° C. However, at 500° C substrate temperature, there is a difference between method A and B, which is shown in Figure 16 and Figure 17. In method A, the same pattern that is obtained with a low substrate temperature is measured, but the method B sample shows the clear diffraction line of the $BaTiO_3$ crystal before the heat treatment. The crystal growth by heat treatment after evaporation, for all the samples take place in the same way as for the samples with low substrate temperature. The change in the diffraction pattern by the heat treatment is compared in Figures 18 - 21, for the method A and B, for various substrate temperatures.

When a quartz plate is used as a substrate, the diffraction line of

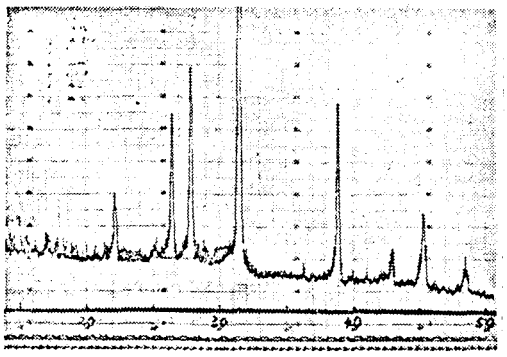

Figure 14

X-ray Diffraction Pattern

M: A S: Pt
S.T: 200°C B.T: 1200°C

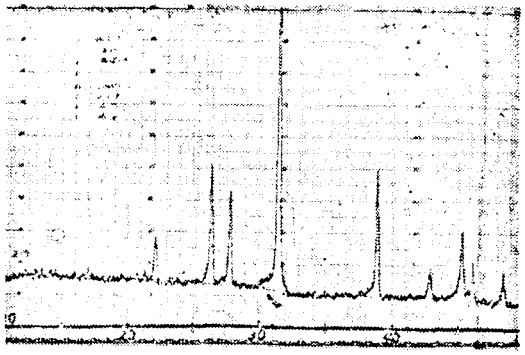

Figure 15

X-ray Diffraction Pattern

M: B S: Pt
S.T: 200°C B.T: 1200°C

the $BaTiO_3$ crystal is not observed by both methods with a 500° C substrate temperature, but it appears with a sample treated at 800° C. Namely, in the case of the quartz substrate, the crystallization temperature is shifted to higher temperatures, as compared to the case of the platinum substrate. Moreover, at the 1,000° C and 1,200° C treatment temperature, due to the diffraction pattern, it is speculated that a compound between $BaTiO_3$ and SiO_2, as well as $BaTiO_3$, is produced.

We shall now consider the size of single crystal grains. This size can be calculated by the width of the diffraction line, by using Scherrer's equation which is:

$$D = \frac{K\lambda}{\beta \cos \theta}$$

D: Size of Crystal Grain

K: Dimensional Factor

β: Spread of the Diffraction Line Width due to the Crystal Size

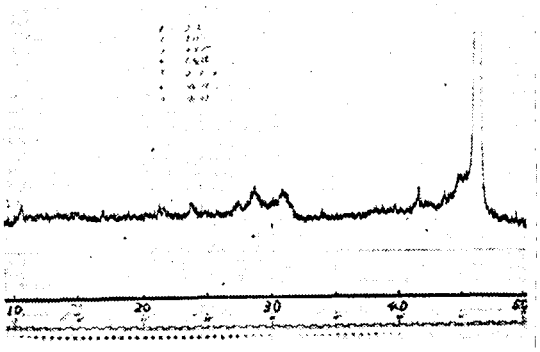

Figure 16

X-ray Diffraction Pattern

M: A S: Pt
S.T: 500°C Untreated

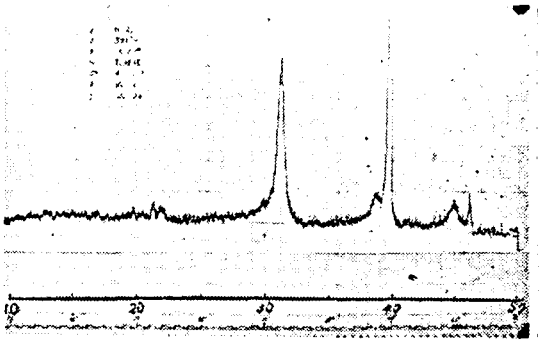

Figure 17

X-ray Diffraction Pattern

M: B S: Pt
S.T: 500°C Untreated

Here, $K = 0.9$ and $\lambda = 1.542$ Å are used on the assumption that the /316 platinum particles are larger than 1,000 Å. The value of β is calculated with the diffraction line of platinum and also with the diffraction line of $BaTiO_3$, corresponding to $2\theta = 31.6^{\circ}$, approximately. The relation between the crystal size and the temperature of the heat treatment is shown in Figure 22. The A and B methods are compared at the substrate temperature of 400° C. The crystals grow with an increase in the treatment temperature, and there is a difference between both methods. This is more remarkable at low temperatures. For example, a result obtained by the B method at 500° C corresponds to that of 700° C by the A method, and no difference is seen at 1,200° C for both methods. In the case when the substrate temperature is 500° C (not in the figure) using the B method, the width of the diffraction line, which appears in the untreated samples, does not change by the heat treatment of the sample in air below 500° C.

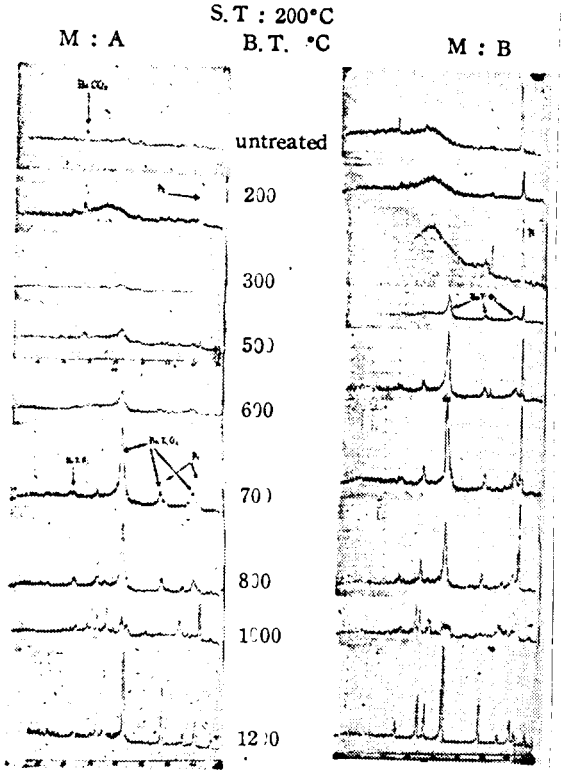

Figure 18

The X-ray Diffraction Pattern of $BaTiO_2$ Films Evaporated by Two Methods

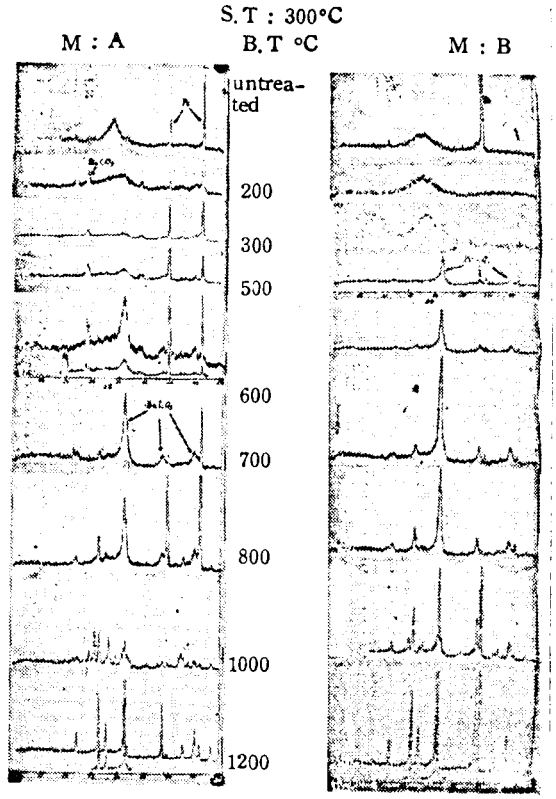

Figure 19

X-ray Diffraction Pattern

/317

There are some substances as well as $BaTiO_3$ in the diffraction patterns. $BaWO_4$ is a possibility, but it was not confirmed in our experiments. The existence of hexagonal $BaTiO_3$, $BaTiO_5$, $BaTi_3O_7$, $BaTi_4O_9$ and Ba_2TiO_4 was also not revealed. (002) and (200) in the cubic crystal around $2\theta = 45^o$ were not separated clearly.

3.3 Optical Density

A stable film can be obtained by method A with a large-capacity, evaporation source heater, which makes the evaporation speed high. Therefore, the samples produced by method A (a temperature increase in 5 seconds to 2.200° C) are used in the following measurements.

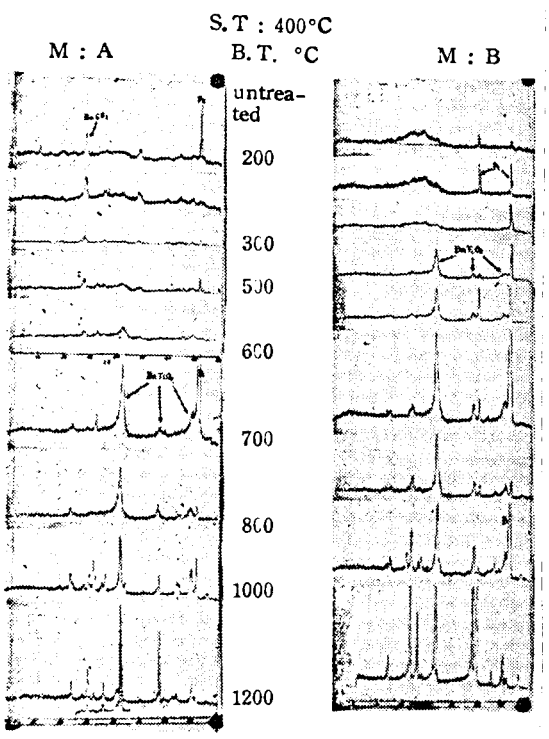

Figure 20
X-ray Diffraction Pattern

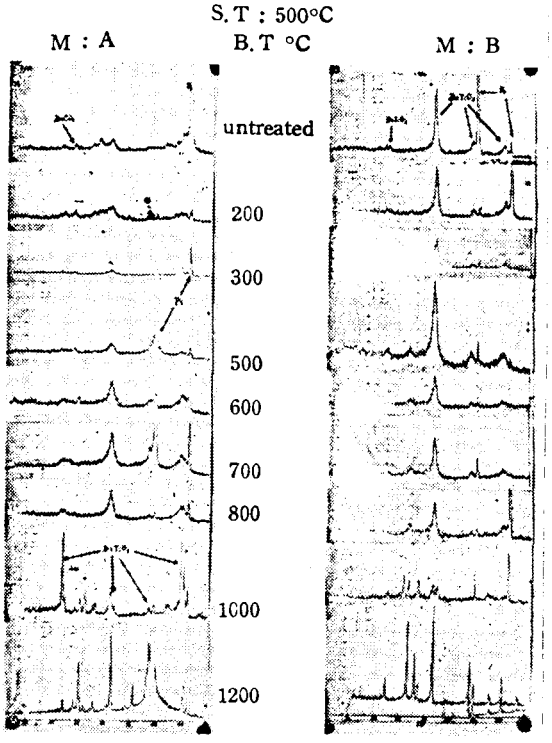

Figure 21
X-ray Diffraction Pattern

The samples are made on the glass substrate with temperatures of 100, 300 and 500° C, and they are measured in the untreated condition. They are next heated at 300° and 500° C in an oxygen atmosphere, and again optically measured. The film thickness is about 1 μ. The measured wave length ranges from 300 mμ to 2.5 μ. The change in the optical density for a sample with the substrate temperature of 500° C is shown in Figure 23. There is no great difference between the untreated and the treated one at 300° C, but the treatment at 500° C makes the optical density fairly low. Almost the same results are obtained for samples whose substrate temperatures are 300° C and 100° C. The color of the film is changed from dark green purple (a lighter shade depends on the heat treatment) to a yellowish

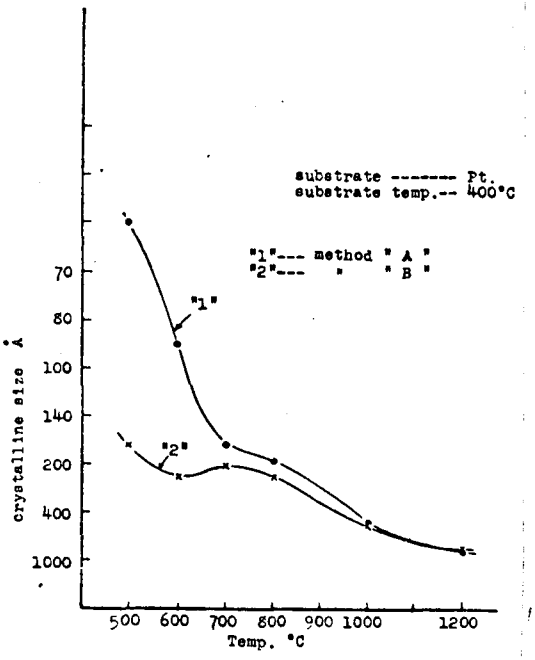

Figure 22

Variation of the Crystalline Size with Baking Temperature

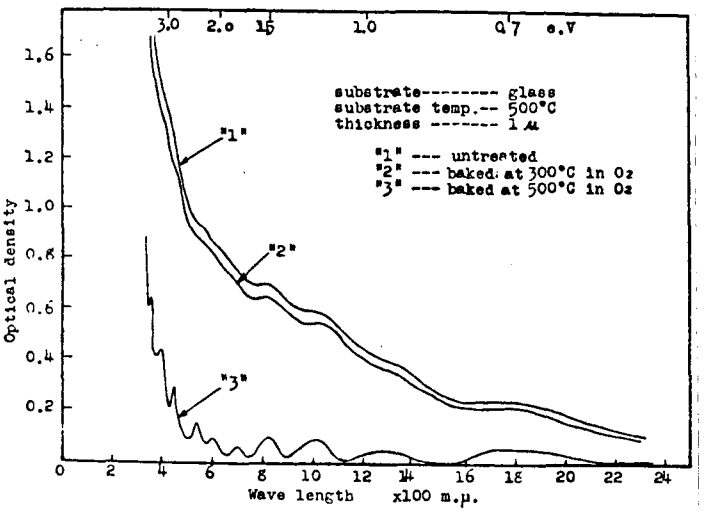

Figure 23

Variation of the Optical Density with Wave Length

transparent color, and the absorption edge becomes clear.

3.4 Electrical Resistance

Electrical conductivity of $BaTiO_3$ becomes great by reduction, and /318 a semiconducting nature appears. Au, Ag, Aℓ are evaporated as electrodes on the films, and D. C. electrical resistances along the surface of the films are measured at temperatures between -170° C and 200° C. The substrate materials are glass, mica and alumina ceramic.

Resistances are small for samples with low substrate temperatures, and the difference in resistance between samples, whose substrate temperatures are 200° C and 500° C, is almost three decades.

A result derived from the resistance measurement with a polished alumina ceramic as substrate is shown in Figure 24. The substrate temperature is

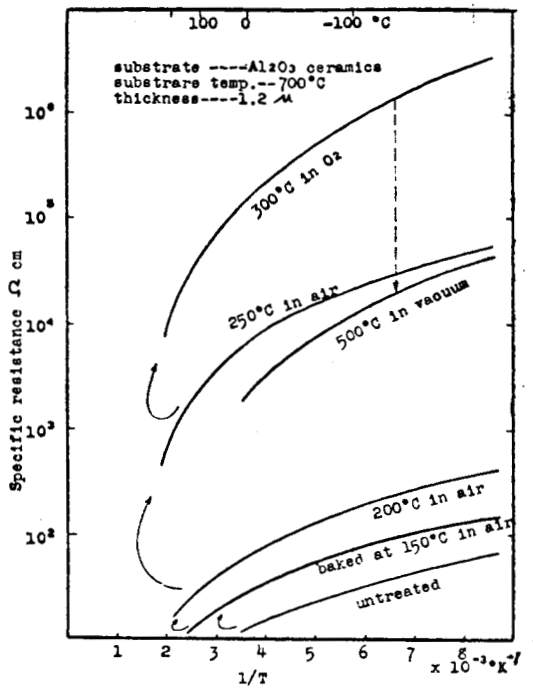

Figure 24

Temperature Dependence of the Specific Resistance

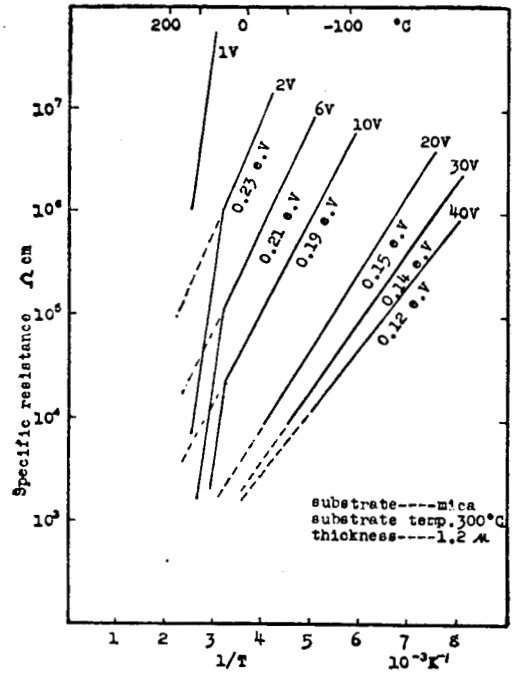

Figure 25

Temperature Dependence of the Specific Resistance

700° C, the film thickness is 1.2 μ. The same sample was heat treated successfully, and was measured from -170° C to 200° C. Heat treatments in air and oxygen after evaporation make their resistance high. When a sample is heated at 300° C in oxygen, its resistance increases, but the resistance again decreases when heated at 500° C in a vacuum. No unusual phenomenon can be observed at about 120° C. The reasons for the resistance increase by the heat treatment are as follows:

(1) Oxidation of the evaporated film;

(2) Crystallization;

(3) Cracking of the film.

The cracking effect may be discarded due to the fact that the reduction

of the film surface again decreases its resistance and that an electron-microscope observation shows no cracking. Film oxidation is most probably the reason. A correlation between the optical property stated above and the electrical characteristic is under consideration.

The dependence of the resistance upon film thickness showed no good results, because the experiment could not be well reproduced.

Some of the high-resistance samples showed non-linear resistance /319 over the applied voltage range. An example - whose substrate is mica, the substrate temperature is 300° C, and the film thickness is about 1 μ - is shown in Figure 25. In this sample, the V-I characteristic shows that the current is proportional to the 4th ~ 5th power of voltage in the range from 1V to 40V. However, the reproducibility is not good.

A solid solution consisting of $SrTiO_3$ and $BaTiO_3$ is tested. Sr concentration is increased from 2% up to 20%, but no significant influence on its nature is observed.

3.5 Dielectric Constant

After the evaporation, the films always have low resistance, regardless of the substrate temperature. The evaporated samples are heat-treated in oxygen or air in order to measure the dielectric constant.

A film is evaporated from a $BaTiO_3$ crystal onto a platinum substrate at 1,200° C substrate temperature, and is heated in air at 1,200° C. The film thickness is about 2 μ. A capacitance value of 4,000 pf is obtained at room temperature with an evaporated Aℓ electrode whose diameter is 1 mm ϕ.

$BaTiO_3$ is easily obtained in hexagonal crystal form when heated in a

reducing atmosphere. The transition reaction from the hexagonal crystal to the cubic crystal takes place very slowly. The produced hexagonal crystal remains in a quasi-stable phase at room temperature. This crystal is not only a ferroelectric, but also prevents the film from showing ferroelectric properties. One method of preventing the formation of the hexagonal crystals was tried by using Sr. This is effective against the hexagonal crystal, but the oxidation process is still required, because of low resistance. A series of experiments was conducted by changing the Sr content, the substrate temperature, the treatment temperature, and the treatment time. Some of the samples can not be measured because of the film cracking and pin-holes. ε-T curves are shown in Figure 26 for some good samples. Temperatures at peaks in curves 1 and 4 are shifted to lower temperatures, as compared to those of the original crystal, and the peaks themselves become broadened. It is assumed that they correspond to the Curie points. In curve 1, two peaks can be seen in the dielectric constant, which suggest two transitions in the low temperature region.

tan δ is about 10% for the samples with large dielectric constant. Blocking voltage is more than 50 KV/cm.

The obvious Curie point is not observed for the other samples. The reasons for the broad peaks in the ε-T characteristic are:

(1) It is measured under a high electric field;

(2) Small crystal particles;

(3) Imperfections in the crystal;

(4) Impurity.

The samples treated at low temperature have small ε and have no change in ε with temperature, as curve 5 in the figure shows. This can be caused

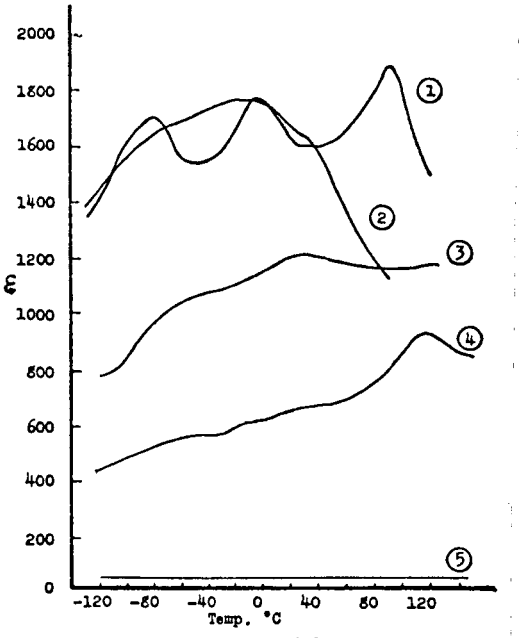

Figure 26

Temperature Dependence of the Dielectric Constant of (Ba-Sr) TiO_3 Films

Sr. %	Thick-ness	S.T.	B.T.	Time	Freq.	E.
1: 5	2.4 μ	500°C	1200°C	2 hr.	30Kc	8.3KV/cm
2:20	2.3	1200	1200	1	10	8.7
3: 0	2.7	700	1200	4	10	7.5
4: 2	3	300	1200	0.5	10	7
5: 0	2.7	300	1000	2	10	7.5

by insufficient oxidation and the hexagonal crystal.

Hysteresis curves for the sample of curve 1 are shown in Figure 27.

In addition, electron micrographs of $BaTiO_3$ films, obtained with /320 platinum substrate at 1000° C and with glass substrate at 500° C, respectively, are shown in Figure 28.

4. Discussion and Problems

First of all, let us consider the result obtained from X-ray diffraction for the evaporated films on the platinum substrates. The following abbreviations are used for purposes of convenience. S.T stands for the substrate temperature during the evaporation; B.T - the baking temperature in air after evaporation.

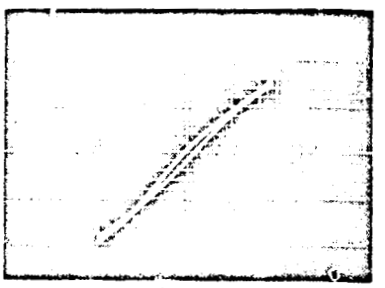

at 26°C

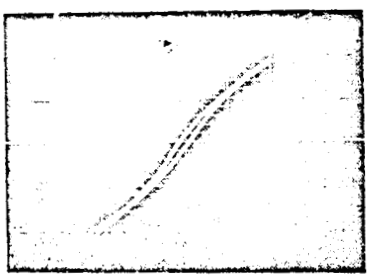

at 100°C

Figure 27

Hysteresis Loop of the Evaporated (Ba·Sr) TiO_3 Films at 50 c/s; the Maximum Applied Field is 17kv/cm

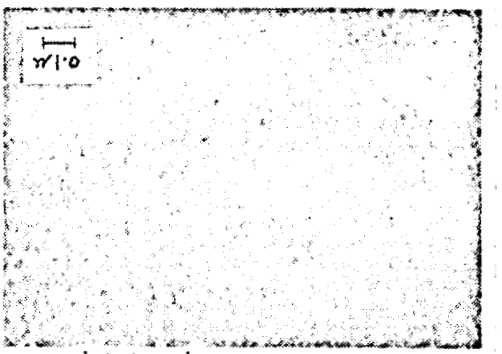

substrate : glass
substrate temp : 500°C

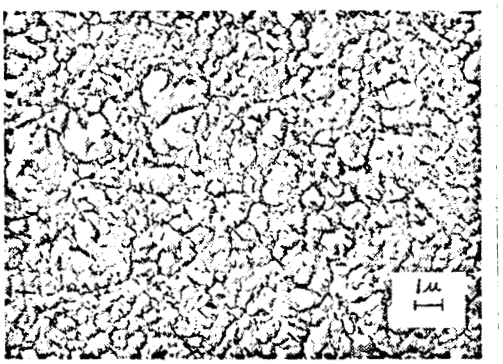

substrate : Pt
substrate temp : 1000°C

Figure 28

Electron Micrographs of the Evaporated $BaTiO_3$ Films (The Pictures are Taken by M. Shibata.)

When $BaTiO_3$ powder is evaporated, the heat treatment has to be done during or after evaporation for both method A and method B, in order to form the $BaTiO_3$ crystals. In both methods, there is a great difference in diffraction line intensity between the sample treated at 300° C and 500° C of the B. T. No experimental point lies in between them, but it is speculated from the experiment on substrate temperature that there is a temperature at which the crystal grows, which can be detected by X-rays, between 400° C and 500° C.

The shape of the diffraction line is also affected by the S.T. Clear lines are observed for the S.T. at 500° C, but they are hardly distinguished for the S.T. below 400° C. On the basis of these results, it is assumed that

a temperature of 500° C is of critical importance for crystal formation. This is not a final conclusion, however, because of insufficient experimental conditions. It is also interesting to note that the crystal condition, with the S.T. at 500° C, and the condition - with the S.T. below 500° C followed by the B.T. at 500° C - show the same structure by X-ray observation. According to a report by Verda (Ref. 6), crystallization progresses at a lower S.T. for a rocksalt substrate. This fact shows that not only the substrate temperature, but also the substrate material have an effect on crystallization.

The difference between the crystal size formed by the heat treatment, using method A and B, is shown in Figure 22. This difference is more pronounced when the B.T. is lower. A treatment at 500° C using method B corresponds to that at 700° C using method A. The difference becomes small above 700° C, and disappears at 1,200° C.

A composite oxide, such as $BaTiO_3$, is assumed to be evaporated by a very complex process, which differs from the evaporation of metals, alloys and compounds, whose vapor pressures are nearly the same. Is it possible that separate molecules in the form of $BaTiO_3$ are present during the evaporation without decomposition? If it once decomposes and vaporizes, the possible combinations are BaO, TiO and a low grade oxide of Ti. Since they have various vapor pressures, the film composition on the substrate changes as a function of time. In general, the form of $Ba_m\ Ti_n\ O_{m+(2n-x)}$ is /321 possible. $Ba_m\ Ti_n\ O_{m+2n}$, which is not a strong dielectric, except for $BaTiO_3$, should be avoided. The reason that $BaTiO_3$ crystallization is easier by method B than by method A, is due to the fact that the composition of the substance on the substrate is almost stoichiometric, and is not changed by

the evaporation time, because of the high evaporation speed. In our experiment, rather small amounts of the crystal were evaporated once, the same procedure had to be repeated five times for a film of 1μ thickness. In method A, the evaporation speed depends on the amount of crystal on the source heater and on heater temperature. At high evaporation speed, method A becomes practically the same as method B. As described in section 3, a stable film was obtained by method A, using a large heater capacity. This can be explained by the reasons noted above.

In this connection, the following method is proposed. Two evaporation sources - one for BaO, and another for TiO_2 - are arranged, and each evaporation speed is controlled independently. This can change the composition and may be useful in a study of the evaporation mechanism.

The diffraction lines around $2\theta=45^{o}$ in the diffraction pattern split into two lines, which are the (002) and (200) ones in the cubic crystal, for material in a natural form. For the evaporated films, on the other hand, no obvious splitting can be observed. There may be a limit to the X-ray diffraction measurement at a film thickness of about 1μ. Under any evaporating condition, the evaporated films show semiconductor-like electrical conductivity, and the resistance decreases by increasing the S.T., and increases with higher B.T.

The dielectric constant is small for the samples with low B.T., and becomes large as the B.T. increases. The dielectric constant for curve 1 in Figure 26 is about the same as with that of $BaTiO_3$ ceramic. But the properties which are different, as compared to the bulk properties, consist of the fact that there is no clear Curie point and the peaks in the dielectric

constant are broad and low. The Curie point of the evaporated films with or without Sr, moves to a lower temperature than that of the original material. In the general case, for ceramics the Curie point moves, depending on the original material and a small amount of impurities. The reasons that the evaporation films have different properties from those of the bulk material are probably: oxygen defects, lattice imperfection, crystal imperfection such as the mixing of micro-size crystals (Ref. 9-12), the mixing of the hexagonal crystals, etc.

These factors are closely related to each other, and several of them are discussed here. First, let us consider insufficient oxygen. Ti oxides can generally be readily reduced in a vacuum, and $BaTiO_3$ is not an exception. Even in a single crystal, the decrease in electrical resistance, when heated in a vacuum, has been reported (Ref. 13). This phenomenon is intensified for the vacuum-evaporated substance, and low resistance films result. $BaTiO_3$ has a tendency to form a hexagonal crystal due to lack of oxygen. This provides a secondary source for the defects. To avoid this, some suitable material should be added to control the atomic valences, or the samples should be heat treated in an oxygen atmosphere after evaporation. The heat treatment has an upper temperature limit because of the substrate used. The problems, therefore, are how to lower the treatment temperature and what kind of treatment should be used in order to obtain the same properties as those of the bulk material.

The addition of Sr was found to be effective in avoiding the formation of hexagonal crystals.

As for the question of the crystal size, the Ps of films is 0.5μ coul/cm^2, according to Feldman. In our experiments, it can be said that Ps is very

small as compared to the value of 26 μ coul/cm^2, for the $BaTiO_3$ single crystal. Impurities are also a possible reason, but even in a single crystal film a few microns thick, the dielectric hysteresis changes considerably (Ref. 14). In ceramics, their dielectric property changes slightly as the crystal size becomes small. It is necessary to determine whether the crystal should have a three-dimensional size larger than a critical value, in order to have the normal and ferroelectric properties. This determination will give a minimum thickness for strong dielectric films.

As one approach toward solving the problem, $BaTiO_3$, (Ba-Sr)TiO_3 and the ceramics powder are melted in a vacuum and oxidized in air. The change in the crystal structure and in the electrical characteristics is being examined at present.

Possible impurities, such as those due to the evaporation heater itself and an agent which is reactive to the original crystal - for example, $BaWO_4$ - should not be introduced. Therefore, the heater must be coated by some suitable material.

Many problems remain, such as: the proper choice of the substrate material with respect to epitaxy condition and thermal expansion, the evaporation speed, the degree of the vacuum, the atmosphere, the effect of the electric field during the evaporation, and more practical parameters - such as the evaporating condition, pinholes, cracking, peeling, the heat treatment, the electrode material, time deterioration, the use of an electron beam for the evaporation, etc.

5. Conclusion

For the $BaTiO_3$ film made by the vacuum evaporation technique, the manner in which the evaporation method, the substrate material, temperature,

and heat treatment affect the $BaTiO_3$ crystal formation was shown. The electrical resistance and the dielectric constant were measured, and future problems were discussed.

With the platinum substrate, the diffraction lines for the $BaTiO_3$ /322 crystal were not observed when the substrate temperature and the treatment temperature were maintained below 400° C. The crystallization proceeds with increasing temperatures.

After the evaporation, the resistance and the dielectric constant are low, regardless of the substrate temperature, and they become higher as the treatment temperature in air is increased.

The $(Ba_{0.95}\ Sr_{0.05})TiO_3$ film (obtained under conditions such as: platinum substrate, 500° C substrate temperature, 1,200° C treatment temperature, 2 hours of treatment time) results in the value of 1,500 for the eielectric constant, and shows three abnormal dielectric constants at 100° C, 0° C and -8° C.

This experiment will be useful as a preliminary study for research on evaporated oxide films.

The authors are indebted to Dr. Hisao Hirabayashi and Dr. Shigeru Waku, Electrical Communication Laboratory, for their kind guidance and advice, and to Dr. Shinichi Niizeki, for his instruction on the X-ray measurement, and also to Mr. Masayuki Itakura and Mr. Shoji Shibata for their help in the experiments.

REFERENCES

1. Feldman, C. Rev. Sci. Instr., 26, 463, 1955; J. App. Phys., 27, 870, 1956.
2. Mool, A. Z. angew. Physik., 10, 410, 1958.
3. Lur'e, M. S. Sov. Phys. Doklady, 4, 1082, 1960.
4. Roder, O. Z. angew. Physik, 12, 323, 1959.
5. Becker, W. M. Bull. Am. Phys. Soc., 4, 184, 1959.
6. Veda, et al. Electronics (Japanese), 7, 90, 1962.
7. Honjo, et al. Meeting of the Physical Society of Japan, April, 1961.
8. Norimoto, et al. Meeting of the Physical Society of Japan, October, 1961.
9. Egerton, L. and Koonce, S. E. J. Am. Cer. Soc., 38, 412, 1955.
10. Hornig, A. W., Rempel, R. C. and Weaver, H. E. J. Phys. Chem. Solids, 10, 1, 1959.
11. Muller, K. A. Helv. Phys. Acta., 31, 173, 1958.
12. Wittels, M. C. and Sherrill, F. A. J. App. Phys., 28, 606, 1957.
13. Toyoda, H. and Itakura, M. J. Phys. Soc. Jap., 17, 924, 1962.
14. Shibata, H. and Toyoda, H. J. Phys. Soc. Jap., 17, 404, 1962.
15. Kay, H. F. and Vousden, P. Phil. Mag., 40, 1019, 1949.
16. Merz, W. J. Phys. Rev., 76, 1221, 1949.
17. Rose, D. E. and Roy, R. J. Am. Cer. Soc., 38, 102, 1955.

Scientific Translation Service
1144 Descanso Drive
La Canada, California